Capacitors with Very Low Loss: Cryogenic Vacuum-Gap Capacitors

Neil M. Zimmerman

Abstract—**We report on measurements of capacitors with about 1 pF of capacitance, which have unmeasurably small leakage at very low frequencies, placing a lower bound of about $10^{19}\Omega$ on the parallel resistance at an effective frequency of 1 mHz. These measurements are made possible by two themes: the use of vacuum-gap capacitors (i.e., no dielectric material, operated in vacuum), and detection of leakage using single electron tunneling (SET) electrometers, which have very high input impedance. We also report on good achieved results in time stability and lack of frequency and voltage dependence.**

I. Introduction and Motivation

THERE are several motivations for the search for capacitors with very high stability, very low loss, and very low frequency and voltage dependence.

For metrologists, one general motivation is that such capacitors allow a better reference to define the absolute value of phase angle. Put another way, they provide a more "pure" capacitance, with less resistive reactance. Using measurements at nonzero frequency, it is very difficult to absolutely define the zero of phase angle, since one can never be sure of the complete absence of any resistive reactance.

There has been previous work on defining an absolute loss angle, θ, and dissipation factor, D, such that $\tan\theta = D = 1/(\omega RC)$, where R and C are in parallel. This work, performed at audio frequencies ($2\pi f = 10^4$ s^{-1}), concentrated on vacuum-gap (room temperature) cross capacitors. In particular, the effects of surface dielectric films were deduced from measurements of electrode separation [1], and by cross-comparison of the capacitance of various combinations of electrodes [2]. These authors assigned uncertainties of about 2×10^{-8} to their measurements of the loss angle. These measurements are difficult and time-consuming, and rely on knowing and accounting for all possible sources of loss.

In contrast, by performing measurements at arbitrarily low frequencies, it is possible to put an arbitrarily large lower limit on the parallel leakage resistance. Thus, an alternative way to define an absolute scale for phase angle or loss, is to work up from such low-frequency measurements. One difficulty in such a procedure is avoiding the finite input impedance of the electrometer. In this paper, we show that extraordinarily high limits on the parallel leakage resistance can be achieved by using SET detectors at low temperatures and low frequencies.

Manuscript received December 11, 1995.

The author is with National Institute of Standards and Technology (NIST), Gaithersburg, MD 20899 USA.

Publisher Item Identifier S 0018-9456(96)06419-4.

A second motivation for studying these capacitors is their potential use as the reference capacitor in temperature dependence measurements of the dielectric constant of various materials. Measurements of the dielectric constant and loss as a function of temperature in many materials yield valuable structural information, such as about two-level systems in glasses. However, the very small amplitude of the temperature dependence sets sharp requirements on the stability, frequency, and voltage dependence, and to a lesser order on the loss of the reference (standard) capacitor [3]. One study [3] in particular developed low-temperature reference capacitors with either excellent stability but poor voltage dependence, or the inverse; the authors could not find a single capacitor satisfying both criteria. Here, acceptable stability and voltage dependence were defined as a relative drift of less than about 10^{-6}/h and dependence of less than 10^{-6}/V, respectively [3]. In this paper, we show that the capacitors described herein come close to or meet both of these criteria.

A final motivation, and the one which is the particular cause for our work in this area, is the recent efforts [4] at NIST to measure absolute capacitance standards using SET pumps [5] and electrometers [6]. These experiments will consist of two different stages: first, we will use a SET pump to deliver a measured number of electrons onto the plate of a stable, low-loss transfer capacitor. Second, we will hold the number of electrons fixed while measuring the voltage (of order 1 V) developed across the capacitor. These two stages will require seconds or tens of seconds to accomplish, and during this time we require that the number of electrons on the capacitor plate remains fixed (within the metrological uncertainty of 10^{-8}). This requirement sets the desired loss, corresponding to a leakage resistance at this "frequency" (really time period) of about 10^{20} Ω. We plan to then compare this transfer capacitance to the unknown or reference standard which is held at room temperature. We thus also require the capacitance of the low-temperature transfer capacitor to be stable over the course of minutes or hours. Since the comparison to the room-temperature capacitor will likely be done at audio frequencies, we also require a very low frequency dependence (or one that is stable and well-characterized) for the transfer capacitance. These requirements are the crucial ones for the transfer capacitor, and here we report our current progress, with lower bound results which are within about a factor of 10 of the requirements for both loss and stability at audio frequencies (with much larger uncertainties at low frequency).

In particular, with the vacuum-gap capacitors, we have observed no drift within our uncertainties, leading to an upper

0018–9456/96$05.00 © 1996 IEEE

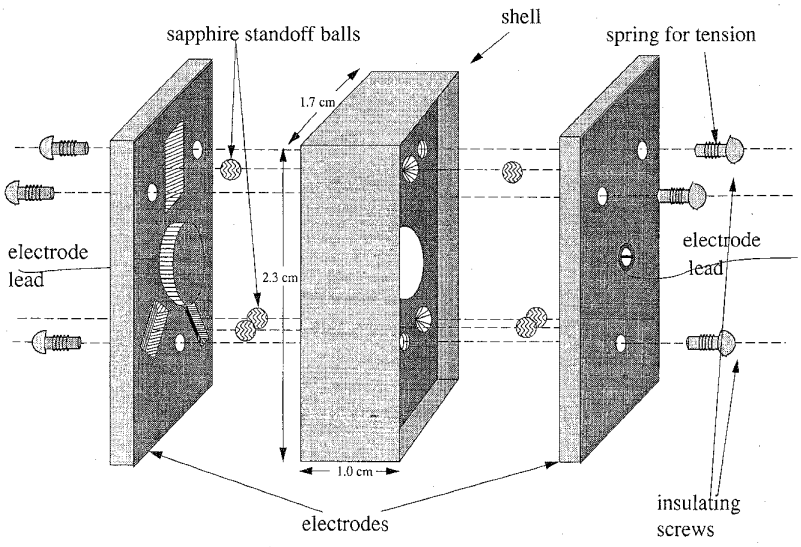

Fig. 1. Exploded view of vacuum-gap capacitors. All three pieces (left and right are the capacitor plates, center is the shell) are machined from copper and the plates are supported by spherical sapphire standoffs. The sapphire balls fit between the grooves in the electrodes and the conical holes in the shell, and provide kinematic support. Set screws between the insulating screws prevent field leakage through the holes. Note that there is no direct physical contact from one electrode to the other; the plates fit into the recesses of the shell. Most of the field lines start at the cylindrical stub projecting from the middle of one electrode, pass through the circular hole in the shell, and terminate at the cylindircal stub on the other electrode; the geometry of this small volume thus mostly determines the value of capacitance. A copper shield surrounds the entire assembled object, with electrical contact with the shell.

bound in the change of capacitance ratios of about 10^{-6} over the course of days. We have also observed no leakage across the capacitor plates, with a best case lower bound of about 10^{19} Ω. This lack of leakage is the main new result of this paper: in contrast, the limits on time stability, and voltage and frequency dependence are useful and important for our work, but not close to those achieved for capacitors used to maintain national standards. These results are achieved with three-terminal capacitors made with copper plates held off from each other by sapphire balls. For comparison, at an effective frequency of about 1 mHz, this corresponds to a loss $D \lesssim 3 \times 10^{-3}$; if, as we believe, the leakage resistance is independent of frequency, at the standard audio frequency of $2\pi f = 10^4$ s^{-1}, the loss $D \lesssim 1 \times 10^{-11}$. These results can be contrasted to earlier measurements made by our group on capacitors made using silica disks coated with metallic electrodes, which had parallel leakage resistances of order 10^{13} Ω [7].

II. Philosophy and Details of Fabrication and Assembly

One of the major difficulties of performing capacitance measurements is the rejection of the stray capacitance to ground from both the leads running to the capacitors, as well as from the capacitor plates themselves. The classic way to avoid this difficulty is to perform a three-terminal capacitance measurement [8]. This scheme consists of two parts. First, all cables and equipment, as well as the plates of the capacitors, are electrostically shielded from the environment by continuous shields; in the case of the cables, this generally means that they must be coaxial. This continuous shield prevents any change in the measured capacitance owing to, for example, movements of wires near the cables. Secondly, the measurement circuit consists of a bridge configuration, with one plate of the each capacitor driven by a low-impedance source, and the other plate connected to the null detector, and thus at a virtual ground. The result of the physical and circuit configurations is to reject any component of the stray capacitance to ground from entering into the measured capacitance; as noted, this includes changes, for example, due to the motion of nearby wires.

In addition to rejecting the effects of capacitance to ground in the leads and plates, the three-terminal measurement also rejects the effects of leakage resistance in these same places. Examples include leakage current through the insulator in coaxial cables and leakage from the capacitor plates to ground. It does not reject any leakage directly from one plate to the other.

We can thus see that the objectives of the three-terminal measurement are a clean definition of the capacitance, and a rejection of parallel resistance. These objectives motivated the design philosophy we have used: we have fabricated three-terminal capacitors, *where each of the plates is mechanically supported only by contact with the grounded shell.* Thus any leakage current through the insulating supports goes only to the grounded shell and is thus rejected in the three-terminal measurement. In addition, the use in vacuum at low temperatures minimizes both the leakage currents and also dielectric loss, which is not intrinsically rejected by this configuration.

An exploded sketch of the capacitors is shown in Fig. 1. The three pieces of metal were machined from OFHC copper. The two plates (left and right pieces) have three triangular grooves which run approximately radially outwards from the center, and the shell (center piece) has three conical holes on each side. This arrangement, with spherical balls placed between the

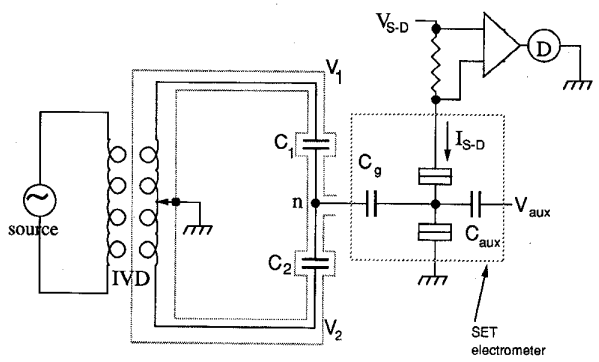

Fig. 2. Electrical circuit for AC bridge measurements. IVD: inductive voltage divider. C_1, C_2: vacuum-gap capacitors. $C_g, C_{\rm aux}$: gate capacitors to SET electrometer. $V_{\rm aux}$: separate voltage applied to auxiliary gate. n: virtual null point when detector D is set to null reading. V_{S-D}: bias voltage applied to electrometer. I_{S-D}: bias current through electrometer (measured signal). The macroscopic elements are all enclosed by the grounded shield as shown. The elements inside the dotted box are microelectronic devices integrated on a Si wafer, and comprise the SET electrometer. D: null detector; this is a lock-in amplifier frequency-locked to the voltage from the source.

plates and the shell, results in a "kinematic" support, with one and only one possible orientation for the plates with respect to the balls. To clamp the plates to the shell, we used insulating screws, and we placed springs on the shafts; by pressing the springs against the plates, we provided a smoother increase in force as we screwed down the bolts, compared to pressing the bolt heads directly against the plates. See the figure caption for further details.

We used sapphire balls for the insulating standoff. Single-crystal sapphire has excellent thermal conductivity at low temperatures, without which it would have been difficult to cool down the plates in a reasonable time. Such balls are routinely used for optical focussing, and are readily available with excellent tolerances on sphericity and absolute size.

To assemble, we first cleaned all parts in an ultrasonic bath of acetone followed by isopropyl alcohol. We then assembled the pieces with gloved hands; with the kinematic support, we did not encounter any difficulties in assembly, even though there are tight tolerances between plate and shell. The cleaning and handling with gloves was done in an attempt to avoid surface organic films on the plates or shell, which could increase the dielectric loss. We found it easiest to handle the small sapphire balls with vacuum tweezers.

We assembled and disassembled the capacitors several times, and found the capacitance value, C, (of order 0.5 pF) repeatable to a level of about 10^{-3} pF. Using different sapphire balls had no discernible effect. In the next design, we plan to incorporate a means of tuning the absolute value C after assembly. This is necessary for the ultimate use in the SET pump experiment, to be able to compare the transfer capacitor to standard capacitors at room temperature.

The assembled plates-plus-shell was then enclosed on all sides in a compartment in a copper box. We made electrical contact to the plates by wires screwed down to the back sides of the plates; these wires ran to coaxial connectors in the sides of the copper box. Coaxial cables then carried the signal up to room temperature. This procedure ensured a continuous electrostatic shield of the two plates, as needed for the three-terminal measurement.

III. Electrical Results

A. Frequency and Voltage Dependences; AC Stability

In this section, we will discuss the results of AC capacitance bridge ratio measurements. The circuit is shown in Fig. 2, and formed a three-terminal bridge, with the two capacitors both being vacuum-gap capacitors as described in Section II. There was one significant difference, however, from conventional bridges: The first stage of the null detector was the SET electrometer, whose bias current, I_{S-D}, was converted to a voltage, and then amplified and demodulated by the lock-in amplifier (LIA), which is part of the detector D. Since an imbalance at point n modulated I_{S-D} through the transconductance of the SET electrometer, the signal out of the LIA was a direct measure of the imbalance in the bridge (i.e., the amount by which C_1/C_2 differs from V_2/V_1). The nominal ratio of the capacitors C_1/C_2 was determined by the ratio of voltages output by the IVD (inductive voltage divider) when point n was at null (i.e., when the null detector reading was lowest, limited by its noise floor).

We note here that we are reporting measurements of the *ratio* of capacitances. Thus, the lack of frequency and voltage dependence, and the time stability, should be viewed only with reference to an imbalance to the two vacuum-gap capacitors, rather than an individual measurement on either. This fact has an important consequence: It is conceivable that these capacitors could, in general, have the identical unwanted behavior (e.g., a drift in time) which would thus cancel in the ratio measurement. For the time stability, we believe such an accidental cancellation to be unlikely, and thus the results reported here are indicative of the performance of each capacitor separately. For the voltage and frequency dependences, such an accidental cancellation is possible (to the level at which the two capacitors are identically constructed), and the results should be viewed in this context.

Three-terminal bridge measurements performed at various voltage source frequencies and amplitudes yield the dependences of the bridge balance on these parameters. We have plotted the results of such measurements in Fig. 3. Here V is the amplitude of the sinusoidal voltage from the source, and is about twice the amplitude of either V_1 or V_2. This plot shows clearly that there was no systematic dependence on frequency or amplitude of applied voltage, within the uncertainties. From these measurements, we can place an upper bound of about 1×10^{-5}/V on the voltage dependence of the ratio measurement.

The smallest uncertainty in the ratio bridge measurements occurred at the largest applied voltage of 10 V peak-peak, with a spread of about 5×10^{-6} in the ratio of C_1/C_2, over the audio frequency range from 100 to 1000 Hz. We note that this spread is simply an upper bound on the true frequency dependence. In addition, crude measurements using DC voltages indicated that the ratio C_1/C_2 was 1.0221 ± 0.0001 at an effective frequency of about 0.01 Hz; thus these very low frequency

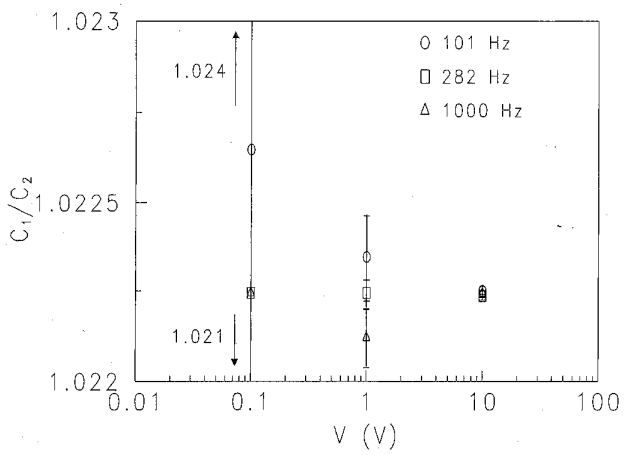

Fig. 3. Frequency and voltage dependence of ratio measurement. We show values for C_1/C_2 as a function of the amplitude of the applied sinusoidal voltage, V, from the source. For each value of V, we made measurements at three frequencies. The error bars shown reflect the fact that the uncertainties scaled roughly with the applied voltage. Note that, within the uncertainties, the ratio was not dependent on frequency or applied voltage amplitude.

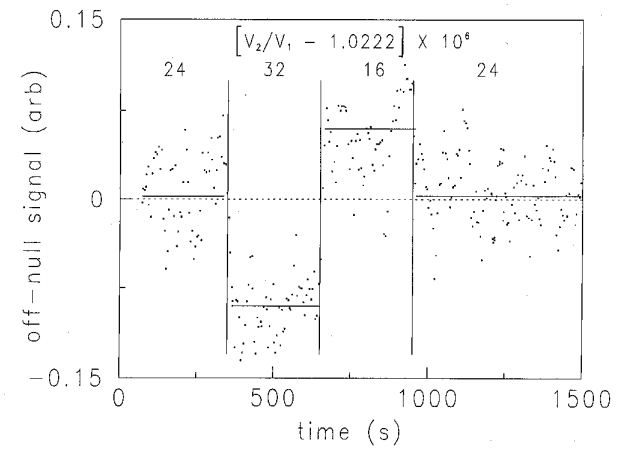

Fig. 4. Time stability of AC bridge ratio measurement. This plot shows the lack of drift for short times of the AC balance of the capacitance ratio bridge measurement. The vertical axis has the output from the null detector, measured at 290 Hz and 10 V peak-peak. The four sections correspond to different settings of the IVD, yielding the shown values of the applied voltages V_1/V_2. The horizontal lines are averages in each of the four regions. The small asymmetry between the two sides of the off-balance is presumably due to a small nonlinearity in the IVD. Note that the first and last sections correspond to nominally identical values of V_1/V_2; the fact that the off-null signal has the same value for these two sections demonstrates that there was no drift in the ratio C_1/C_2 over the 1500 s shown.

measurements also indicate no frequency dependence over the entire frequency range within the much larger uncertainty of 10^{-4}. We will continue to decrease uncertainties in the frequency and voltage dependences in the next round of measurements.

To demonstrate the stability in time of these capacitors at audio frequencies, we fixed the IVD setting, and monitored the imbalance signal from the null detector (LIA output). For short times, we then digitized the observed signal as a function of time. An example is shown in Fig. 4. Here we have four sections of approximate duration 300 s each, with different

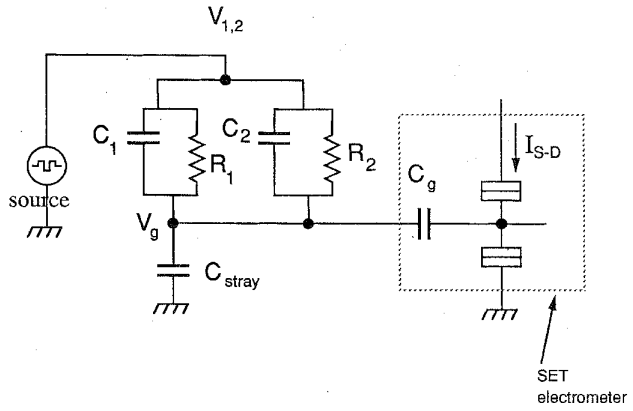

Fig. 5. Electrical circuit for the capacitor leakage measurements. Here, both vacuum-gap capacitors C_1 and C_2 are connected in parallel, with the same voltage $V_{1,2}$ applied to both. Any possible leakage in the capacitors is represented by the parallel resistances R_1 and R_2 as shown, and will result in a slow drift in V_g, after the application of an abrupt change (a "switch") in $V_{1,2}$. As described in the text, the size of this drift depends on the size of the stray capacitance to ground, C_{stray}, between the vacuum-gap capacitors and the SET electrometer (in the dotted box). A possible drift in V_g is measured by a drift in the current output, I_{S-D}, of the electrometer.

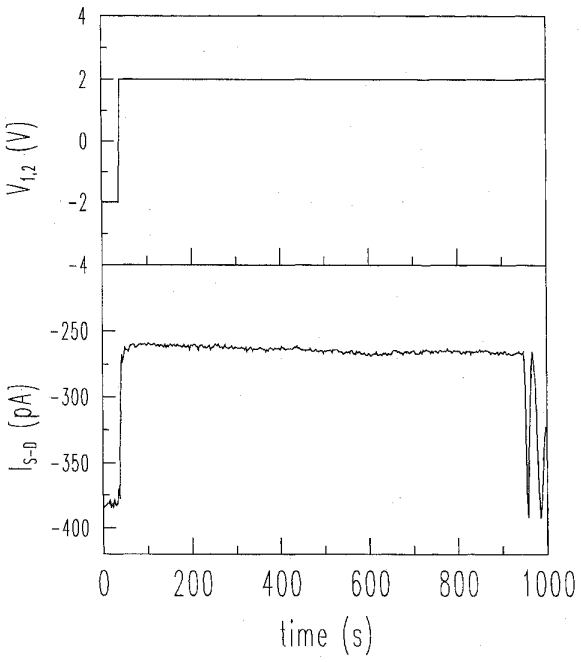

Fig. 6. Results of a switching experiment. Upper panel is the voltage $V_{1,2}$ as a function of time, with one switch at 50 s, and a slow ramp from 950 to 1000 s. Bottom panel is the electrometer output I_{S-D} over the same time interval. The abrupt change in I_{S-D} at 50 s is the result of the switch in $V_{1,2}$. The oscillations from 950 to 1000 s are the result of the ramp in $V_{1,2}$, and show the dependence $I_{S-D}(V_{1,2})$, including the full range of the oscillation. Note that, between 50 and 950 s, I_{S-D} has essentially no time dependence (detailed analysis of the data indicates that the slight slope is mostly due to a small drift in $V_{1,2}$). This lack of time dependence shows the lack of any leakage resistance in the capacitors, and the lack of any drift in the value $C_1 + C_2$.

settings on the IVD corresponding to the ratios shown. We can see that, over the course of the 300 s for a single section, as well as the total duration of 1200 s, the balance point (and thus

TABLE I
LOWER AND UPPER BOUNDS ON FREQUENCY AND VOLTAGE DEPENDENCE, TIME STABILITY, AND LEAKAGE RESISTANCE OF VACUUM-GAP CAPACITORS. SHORT-TERM RESULTS (dC_1/dt) ARE FROM CONTINUOUS MEASUREMENTS AS IN FIGS. 4 AND 6. LONG-TERM RESULTS ($\delta(C_1/C_2)/\delta t$) ARE FROM REPEATED SINGLE MEASUREMENTS OVER A COURSE OF WEEKS. THE CAPACITORS HAVE ABSOLUTE VALUES OF ABOUT 0.5 pF. DC REFERS TO MEASUREMENTS OVER PERIODS RANGING BETWEEN 100 s AND 1000 s

Quantity	Frequency Range	Result
frequency dependence	audio (100 Hz to 1000 Hz)	$\delta(C_1/C_2) < 5 \times 10^{-6}$
	audio to DC	$\delta(C_1/C_2) < 1 \times 10^{-4}$
voltage dependence	audio	$\delta(C_1/C_2)/\delta V < 1 \times 10^{-5}$/V
time stability	audio	short-term $d(C_1/C_2)/dt < 1 \times 10^{-5}\text{h}^{-1}$
		long-term $\delta(C_1/C_2)/\delta t < 1 \times 10^{-8}\text{h}^{-1}$
	DC	short-term $dC_1/dt < 4 \times 10^{-4}$ pF/h
		short-term $1/C_1 dC_1/dt < 8 \times 10^{-4}$ h^{-1}
		long-term $\delta(C_1/C_2)/\delta t < 1 \times 10^{-6}\text{h}^{-1}$
leakage resistance	DC	$\text{R} > 1 \times 10^{19}\Omega$

the ratio C_1/C_2) is unchanged (note that the first and last IVD ratios are the same). With an upper bound for the change in C_1/C_2 of about 4×10^{-6}, we can thus assign an upper bound for the short-term stability of $d(C_1/C_2)/dt \lesssim 1.0 \times 10^{-5}$ h^{-1}. For longer times, we observed the balance point and any changes at fixed frequency and voltage, over a period of two weeks. We observed a spread of values of 2×10^{-6}, with no systematic drift, over a period of 12 days. These measurements were performed at 280 Hz and 10 V peak-peak. *We thus assign an upper bound of about* 1×10^{-8} h^{-1} *to the long-term drift* in C_1/C_2, *at audio frequencies.*

B. Leakage Resistance; DC Stability

In this section, we will examine the leakage (dissipation) at very low frequencies; these results will also yield bounds on the drift in $C_1 + C_2$ at low frequencies. To measure the leakage (or put a lower bound on the parallel leakage resistance), we used a circuit as shown in Fig. 5. The source is either an electrochemical battery whose output is manually switched, or a digital source. The two vacuum-gap capacitors are connected in parallel, as shown, with possible leakage resistances denoted as R_1 and R_2. After the imposition of an abrupt change (a "switch") in $V_{1,2}$, a finite value for R_1 or R_2 or equivalently a drift in dC/dt ($C \equiv C_1 + C_2$) will result in a drift in V_g, and thus a drift in the electrometer output, I_{S-D}. We have also indicated the stray capacitance to ground between the capacitors and electrometer, C_{stray}, since it is important for the analysis.

We will now do the calculation necessary to estimate R_1, R_2, and dC/dt from changes in I_{S-D}. For the data discussed below, we have estimated (based on other measurements) C_{stray} to be approximately 40 pF. This value is much greater than in our previous work [7], and is due to the close spacing of the plates to the ground shell. This large value is undesirable, since a larger C_{stray} decreases the sensitivity of the bridge balance measurement. In the next design, we will rectify this weakness, while maintaining adequate isolation between the two plates.

Thus C_{stray} is much greater than C_1, C_2, C_g, or the other capacitances in the electrometer, which implies that $V_g \ll V_{1,2}$. Thus we can set $V_g = 0$ initially. Then, after a switch to a value V for $V_{1,2}$, the effect of parallel resistance is that a leakage current I develops: $I = V/R$, where we have assumed $R_1 = R_2 = 2R$. Since C_{stray} is much greater than the capacitances in the electrometer, we have

$$dV_g/dt = I/C_{\text{stray}} \approx V/(RC_{\text{stray}})$$

or

$$R \approx V/C_{\text{stray}}(dV_g/dt)^{-1}. \tag{1}$$

Similarly, a drift dC/dt in $C = C_1 + C_2$ will manifest itself as follows

$$V_g \approx (C/C_{\text{stray}})V \Rightarrow dV_g/dt \approx V(dC/dt)/C_{\text{stray}}$$

or

$$dC/dt \approx C_{\text{stray}}(dV_g/dt)/V. \tag{2}$$

To use this analysis, we examine data of the type shown in Fig. 6. The upper panel shows the time dependence of $V_{1,2}$: A switch, followed by a long constant period, and then a small ramp (barely visible in the figure) at the end. The lower panel shows the corresponding time dependence of I_{S-D}: A switch at the same time as $V_{1,2}$, a long mostly constant period, and the oscillations at the end, due to the ramp in $V_{1,2}$. These oscillations show the behavior of the electrometer transconductance, $I_{S-D}(V_g)$ or $I_{S-D}(V_{1,2})$, and allow us to calibrate any changes in I_{S-D} over the time period. We note that we have made many measurements of the type shown in Fig. 6; some of these show as little drift in I_{S-D}. Others show substantial time dependence, but not the

linear time dependence which would be exhibited by a parallel resistance, as shown in (1). Instead, the time dependence is the random noise or discrete switching behavior commonly observed in the SET electrometer [9]. *We have never observed the monotonic time dependence of V_g which would result from parallel leakage resistance.*

Thus, we can examine the data in Fig. 6 to set lower and upper bounds on R and dC/dt, respectively. A detailed analysis of the data in Fig. 6 indicates that most of the small amount of drift observable in I_{S-D} between 50 s and 950 s is due to drift in the battery-imposed $V_{1,2}$ as measured by a precision voltmeter. We can set an upper bound on the intrinsic change in I_{S-D} over this time period as corresponding to a change in the gate voltage of $0.03\Delta V_G$ (ΔV_G is the period in voltage of one oscillation), or $\delta V_g \lesssim 0.010$ mV over 900 s. If we attribute this to a linear drift in V_g, we can assign an upper bound of $dV_g/dt \lesssim 0.010$ mV/900 s. From (1), this puts a lower bound on the resistance of $R \gtrsim 5 \times 10^{18}\ \Omega$, or a *lower bound on the parallel leakage resistance of one capacitor* R_1 or $R_2 \gtrsim 10^{19}\ \Omega$. Similarly, from (2), we can put an upper bound of $dC/dt \lesssim 8 \times 10^{-4}$ pF/h, or $dC_1/dt \lesssim 4 \times 10^{-4}$ pF/h. This corresponds to a time stability $1/C_1\ dC_1/dt \lesssim 8 \times 10^{-4}\ \mathrm{h}^{-1}$ at very low (of order 1 mHz) frequencies. In addition, similar to the audio frequency measurements, we also performed multiple low-frequency bridge ratio measurements, with a spread in the values of C_1/C_2 of 3×10^{-4} over the course of 11 days, corresponding to an upper bound on long-term drift of $\delta C_1/\delta t \lesssim 1.1 \times 10^{-6}\ \mathrm{h}^{-1}$.

IV. Conclusion

The various parameters we have been able to place on these simple custom-fabricated vacuum-gap capacitors are listed in Table I. We can see that, in general, the time stability and lack of frequency and voltage dependence makes these capacitors attractive candidates for the reference capacitors in low-temperature dielectric constant and loss measurements [3].

We can also see that, although the lower bound on the parallel resistance is about one million times larger than the previous attempt [7], we have not yet demonstrated that the loss in these capacitors is sufficiently small to make them acceptable for the SET pump-charging experiment [4], which will require resistances in excess of $10^{20}\ \Omega$.

Our next steps will focus on two important goals. The first is to demonstrate bridge ratio measurements with uncertainties of no more than 10^{-8} in C_1/C_2, and resistances of at least $10^{20}\ \Omega$. The second goal is to design these capacitors with lower capacitance to ground, C_{stray}, and with the ability to tune C_1 to within 10^{-4} pF of a nominal value. This latter goal may require the tuning to be performed at operating (cryogenic) temperatures, because the change in C_1 from room temperature may not be predictable to this level.

Acknowledgment

The author would like to thank E. R. Williams for the initial suggestion and continuing advice, and K. E. Lease for assistance in the initial assembly and testing of the capacitors. He also acknowledges the technical assistance of W. Fogle, A. F. Clark, and R. J. Soulen in the low-temperature measurements, and a useful discussion regarding electrode cooling with F. Wellstood.

References

[1] E. So and J. Q. Shields, *IEEE Trans. Instrum. Meas.,* vol. IM-28, p. 279, 1979.
[2] J. Q. Shields, *IEEE Trans. Instrum. Meas.*, vol. IM-27, p. 464, 1978.
[3] M. C. Foote and A. C. Anderson, *Rev. Sci. Instrum.,* vol. 58, p. 130, 1987.
[4] E. R. Williams, R. N. Ghosh, and J. M. Martinis, *J. Res. NIST,* vol. 97, p. 299, 1992.
[5] J. M. Martinis, M. Nahum, and H. D. Jensen, *Phys. Rev. Lett.,* vol. 72, p. 904, 1994; M. W. Keller, J. M. Martinis, N. M. Zimmerman, and A. H. Steinbach, *Appl. Phys. Lett.,* to be published.
[6] A. F. Clark, N. M. Zimmerman, E. R. Williams, A. Amar, D. Song, F. C. Wellstood, C. J. Lobb, and R. J. Soulen, Jr., *Appl. Phys. Lett.*, vol. 66, p. 2588, 1995.
[7] R. N. Ghosh, A. F. Clark, B. A. Sanborn, and E. R. Williams, *Coulomb and Interferene Effects in Small Electronic Structures.* Gif-sur-Yvette, France: Frontier, 1995, p. 173.
[8] B. P. Kibble and G. H. Rayner, *Coaxial AC Bridges.* Bristol, U.K.: Adam Hilger, 1984.
[9] G. Zimmerli, T. M. Eiles, R. L. Kautz, and J. M. Martinis, *Appl. Phys. Lett.,* vol. 61, p. 237, 1992.

Neil M. Zimmerman was born on June 21, 1960. He received the B.S. degree in physics from Rensselaer Polytechnic Institute, Troy, NY, in 1982, and the M.S. and Ph.D. degrees in physics from Cornell University, Ithaca, NY.

He was a postdoctoral associate at AT&T Bell Labs from 1989 to 1992, and as a research physicist at the Naval Research Lab from 1992 to 1994. He is currently employed as a research physicist in the Fundamental Electrical Measurements Group, National Institute of Standards and Technology, Gaithersburg, MD, where he works on applications of single electron tunneling devices for standards of electrical capacitance or current.